ELSEVIER

Journal of Nuclear Materials 290–293 (2001) 1102–1106

journal of nuclear materials

www.elsevier.nl/locate/jnucmat

Material degradation and particle formation under transient thermal loads

J. Linke [a,*], M. Akiba [b], R. Duwe [a], A. Lodato [a], H.-J. Penkalla [a], M. Rödig [a], K. Schöpflin [a]

[a] *Forschungszentrum Jülich, EURATOM Association, IWV-2, D-52425 Jülich, Germany*
[b] *Naka Fusion Research Establishment, JAERI, 801 Mukoyama, Naka-machi, Ibaraki-ken 311-01, Japan*

Abstract

Carbon-based materials and metals have been exposed to fusion relevant thermal loads in an electron beam test facility to simulate off-normal plasma conditions such as disruptions or vertical displacement events (VDEs). The erosion process in carbon-based materials is dominated by brittle destruction, a process which is associated with the formation of carbon dust; this process becomes essential at a threshold value of approx. 200 MW m^{-2}. In metals the dominating processes are melting, crack formation in the recrystallized material, and – at higher thermal loads – splashing and boiling of the melt layer. Additional material degradation due to neutron irradiation (up to 0.35 dpa at 350°C and 700°C) and its influence on the high heat flux performance have been investigated.

Keywords: Thermal load

1. Introduction

Plasma facing components in future confinement experiments will be subjected to transient heat fluxes during off-normal plasma scenarios. In these events the thermal load will be deposited on local surface areas with energy densities up to several ten megajoules per square meter [1,2]. Heat loads are $\leqslant$150 MJ m^{-2} within a few milliseconds during disruptions and $\leqslant$60 MJ m^{-2} for approx. 0.1 s during vertical displacement events (VDEs).

2. Simulation experiments

To investigate the performance of different plasma facing materials, high heat flux simulation experiments have been performed in electron beam test facilities with scanned and defocussed electron beams. Here thermal loads with parameters relevant for next step fusion devices have been applied to metals (different beryllium grades, tungsten alloys) and carbon-based materials (fine grain graphites, carbon fiber composites). Extensive diagnostics such as beam current and calorimeteric measurements have been used to characterize the energy input, the thermal response of the test samples, and the resulting material degradation. Special attention was given to the analysis of particles which were generated during electron beam loading.

The material response during electron beam loading is shown schematically in Fig. 1 for metals and carbon-based materials.

3. Results

Unlike the conditions in a thermonuclear fusion device, the electron beam deposits its energy in the volume of the plasma facing material. The penetration depth depends strongly on the acceleration voltage

* Corresponding author. Tel.: +49-2461 61 3230; fax: +49-2461 61 3687.
E-mail address: j.linke@fz-juelich.de (J. Linke).

0022-3115/01/$ - see front matter
PII: S0022-3115(00)00547-X

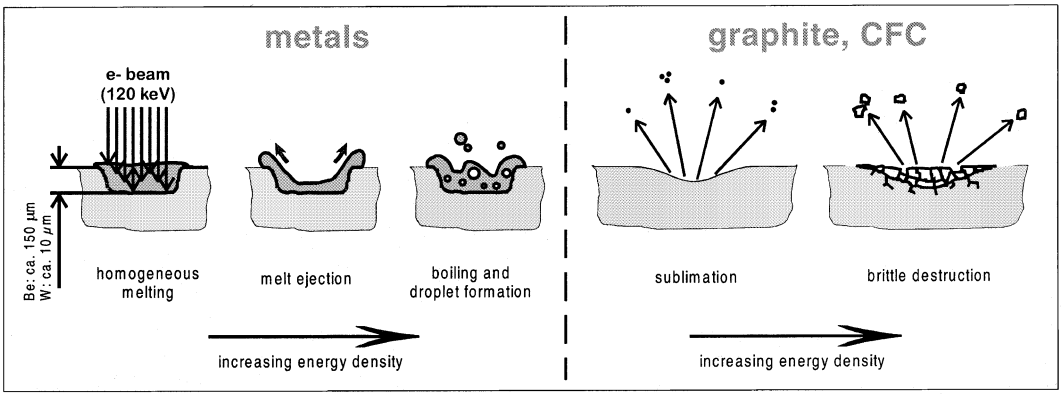

Fig. 1. Thermal loading of metals and carbon-based materials with intense localized electron beams. Due to the energy of the incident electrons (typically 120 keV, a volumetric heat deposition occurs in a depth of approx. 150 μm in Be or C, and approx. 10 μm in W.

($U = 120$ kV) and on the density of the material; it is in the order of 150 μm for Be or C, and about 10 μm for W. For beam currents below 19 mA, i.e., for power densities below approx. 200 MW m^{-2} evaporation of carbon atoms or small atomic clusters is the major erosion mechanism for fine grain graphites, cf. Fig. 2. Due to the better thermal conductivity this threshold value is lower for CFC materials.

When this critical electron beam current is exceeded, the sublimation dominated erosion is succeeded by a

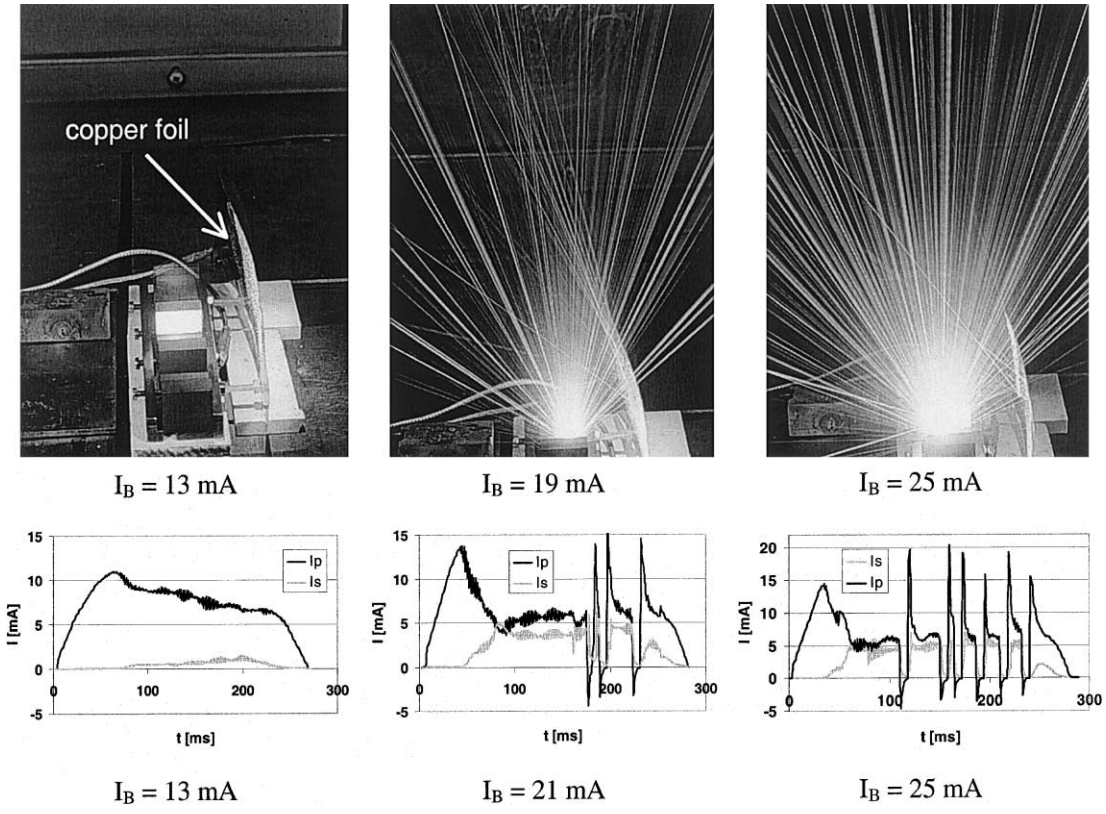

Fig. 2. Electron beam loading of graphite EK 98, $U_B = 120$ kV, $\Delta t = 0.2$ s; top: particle emission starts at about 19 mA, bottom: current of the absorbed and reflected electrons (I_B = incident beam current, I_P = current through the sample, I_S = current absorbed by an isolated copper foil).

new process, namely the emission of particles [3] from the electron beam loaded surface, a phenomenon which is in general described as 'brittle destruction' [4]. Particles originating from this process have been collected and analyzed using optical and electron microscopy. The size of these objects shows maximum values of approx. 100 μm. In addition, tiny spherical objects with diameters of 0.01 μm have been detected by TEM analysis, obviously fullerenes or nanotubes which are generated during intense thermal loads. These objects coagulate to form larger agglomerates with dimensions of a few hundred nanometers [5]. The intensity of particle generation depends on the type of carbon material. There is some indication that the process of brittle destruction is generally less developed for carbon grades with a higher thermal conductivity.

The current absorbed by the graphitic test sample during electron beam loading I_P is plotted in the bottom of Fig. 2. It decreases continuously during the 200 ms beam pulse; simultaneously I_S, the current absorbed by an isolated copper foil, which originates from reflected and thermionic electrons, increases permanently. For incident beam currents above the threshold value ($I_B \geqslant 19$ mA) both signals (I_P and I_S) show strong fluctuations which are caused by carbon particles which penetrate into the beam generation system and cut off the beam temporarily.

Electron beam loading of metals at 'moderate' energy densities (up to a few MJ m^{-2}) will result in a homogeneous, localized melting of the sample surface. After resolidification and further cool down below the ductile–brittle transient temperature (DBTT) of the test coupon the sample will undergo severe cracking [6]. When higher energy densities are applied, surface evaporation becomes essential; the momentum transfer due to evaporating atoms from the surface generate an effective pressure on the melt layer which finally results in the ejection of melt from the crater (cf. Fig. 1). As can be seen in metallographic sections from erosion craters on tungsten in Fig. 3, the depth of the crater increases from 0.3 to 1.2 mm when the test sample is preheated to 650°C before the experiment. Both samples have been exposed to 10 identical beam pulses with an energy density of 2.3 MJ m^{-2} ($\Delta t = 1.8$ ms) in the electron beam facility JEBIS at JAERI, Japan. The evaporation losses for the preheated sample are a factor 8 larger. This test sample shows a well-pronounced crater rim originating from the melt ejection from the central crater region. The remaining melt layer at the bottom of the crater also shows a reduced thickness. These findings are attributed to the higher momentum transfer to the melt layer and hence, result in a stronger melt ejection. In addition, cracks which penetrate deep (crack length $\leqslant$ 1 mm) into the bulk material have only been observed on the room temperature sample. Only a rather thin surface layer is heat affected during the short (1.8 ms) beam pulse. Hence, the major fraction of the material is below DBTT and remains brittle. The preheated sample

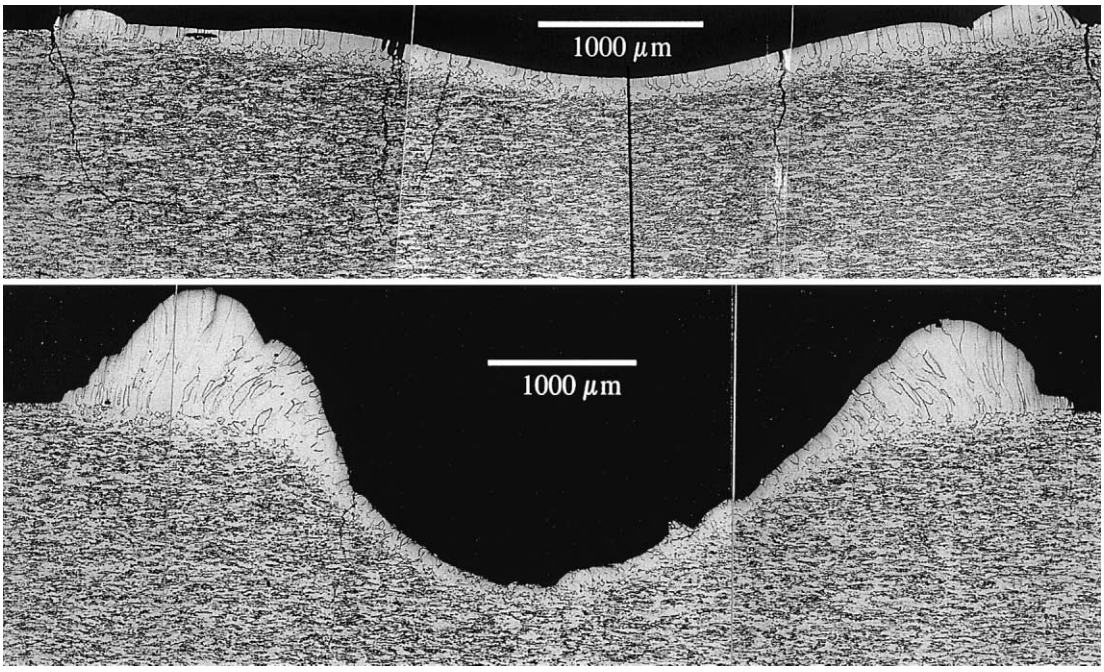

Fig. 3. Electron beam loading of tungsten at different sample temperatures: $E_{inc} = 2.3$ MJ m^{-2}, $\Delta t = 1.8$ ms, 10 shots; top: non-preheated sample, weight loss = 0.5 mg, bottom: sample pre-heated to 650–700°C, weight loss = 4.0 mg.

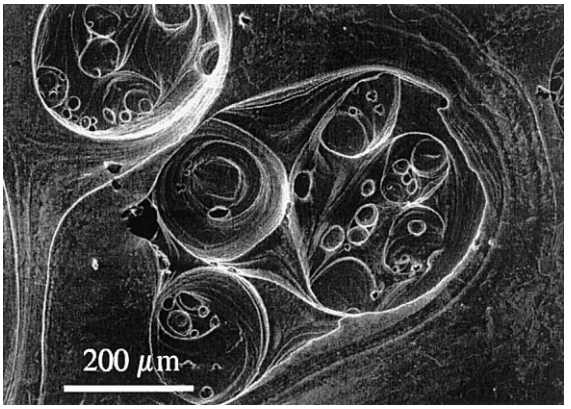

Fig. 4. Formation of gas bubbles during electron beam loading of titanium: $U_{acc} = 120$ kV, $I_{inc} = 300$ mA, $\Delta t = 5$ ms, 1 shot, defocused beam.

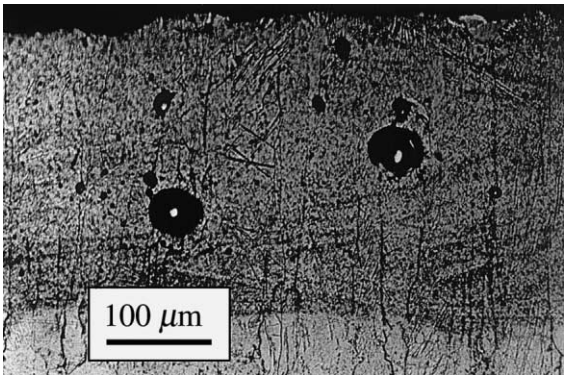

Fig. 5. Pore formation during electron beam loading of neutron irradiated beryllium (DShG 200, $T_{irr} = 700$°C, $\phi = 0.35$ dpa): $I_{inc} = 400$ mA, $\Delta t = 5$ ms, 5 shots.

($T >$ DBTT) does not show any cracks since the material behaves ductile.

Increasing the incident energy density results in an intense boiling and convection of the melt layer [7]. To study this phenomenon a selection of different metals have been subjected to beam pulses of about 10 MJ m^{-2} for 5 ms. Under these conditions bubbles and open pores are evident in the recrystallized surface layer (e.g., in titanium samples, cf. SEM-micrograph in Fig. 4).

To investigate the effect of neutron irradiation on the material performance, test coupons from ITER relevant plasma facing materials have been exposed to neutron fluxes of 0.35 dpa ($T = 350$°C and 700°C, respectively) in the high flux reactor (HFR) in Petten.

The erosion behavior of the irradiated test coupons has been compared with un-irradiated test specimens. Carbon fiber composite show an increased material erosion ($E_{inc} = 8.4$ MJ m^{-2}, $\Delta t = 5$ ms) for the lower irradiation temperature; at $T_{irr} = 700$°C the effect is less pronounced.

These findings have been reported by other authors as well [8]; they are mainly due to the irradiation induced degradation of the thermal conductivity; at elevated temperatures part of the radiation damage has been recovered.

For beryllium a similar effect, i.e., an increased erosion after neutron irradiation (up to 100%) has been measured as well. This process cannot be attributed to a decrease in the thermal conductivity of the bulk beryllium. However, a clear pore formation has been observed in the melt layer of all neutron irradiated test coupons after electron beam loading, Fig. 5. The tritium and helium production due to neutron irradiation in the HFR reactor at 700°C has been calculated to be 1.7×10^{16} and 3.6×10^{18} atoms/g Be, respectively, which corresponds to a total concentration of 55 ppm. During disruptions these gases will form bubbles in the melt layer. In Be the neutron-induced embrittlement and thermally induced cracks during electron beam loading with transient heat pulses may also play a non-negligible role.

4. Conclusions

The erosion of carbon-based materials during severe thermal shocks (disruptions, VDEs) is dominated by brittle destruction which may result in the formation of dust particles (graphitic grains or clusters of carbon fibers) with diameters up to 100 μm. For graphites this process becomes essential at a threshold value of approx. 200 MW m^{-2}. In CFCs with improved thermal conductivities the material erosion due to brittle destruction is reduced.

Metals, particularly beryllium, will melt under disruption or VDE heat loads; in addition, an intense crack formation has been observed. Similar effects have been studied for tungsten at energetic electron beam pulses with pulse durations of a few milliseconds; however, due to the high melting temperature the formation of a melt layer and crack initiation becomes only essential at higher energy densities. For base temperatures above DBTT the crack formation can be neglected for tungsten. In beryllium the tendency to from cracks is also reduced at elevated temperatures. As long as evaporation losses are negligible, the electron beam heating will result in the formation of a homogeneous melt layer. At increased energy densities this layer becomes unstable; the melt is ejected form the crater region resulting in deep craters with a rim of resolidified material. A further increase of the beam energy finally results in the boiling of the melt layer; this process is associated with the formation or metallic droplets.

Neutron irradiation results in an additional material damage. Carbon materials show an increased erosion due to a reduction in the thermal conductivity. In

beryllium the formation of pores in the resolidified melt layer due to the release of He and tritium could have a significant influence on the thermal transport through this layer.

References

[1] A. Hassanein, G. Federici, I. Konkashbaev, A. Zhitlukhin, V. Litunovsky, Fusion Eng. Des. 39–40 (1998) 201.
[2] M. Merola, M. Rödig, J. Linke, R. Duwe, G. Vieider, J. Nucl. Mater. 258–263 (1998) 653.
[3] J. Winter, G. Gebauer, J. Nucl. Mater. 266 (269) (1999) 228.
[4] J. Linke, H. Bolt, P. Chappuis, H.J. Penkalla, M. Scheerer, K. Schöpflin, in: Proceedings of the 5th International Symposium on Fusion Nuclear Technology, Rome, 19–24 September 1999.
[5] Ph. Chappuis, E. Tsitrone, M. Mayne, J. Linke, H. Bolt, D. Petti, J.P. Sharpe, these Proceedings.
[6] J. Linke, R. Duwe, A. Gervash, R.H. Qian, M. Rödig, A. Schuster, J. Nucl. Mater. 258 (1998) 634.
[7] K. Nakamura, S. Suzuki, T. Tanabe, M. Dairaku, K. Yokoyama, M. Akiba, Fus. Eng. Des. 39 (1998) 295.
[8] M. Uda, E. Ishitsuka, K. Sato, M. Akiba, C. Yamamura, S. Takebayashi, H. Kawamura, in: Proceedings of the 20th Symposium on Fusion Technology, Marseille, 7–11 September 1998, p. 161.